ELECTRON-CLOUD BUILD-UP SIMULATIONS AND EXPERIMENTS AT CERN

G. Arduini, V. Baglin, T. Bohl, B. Jenninger, J.M. Jimenez, J.-M. Laurent,
F. Ruggiero, D. Schulte, F. Zimmermann, CERN, Geneva, Switzerland

Abstract

We benchmark the predictions of electron-cloud build-up simulations against measurements at the CERN SPS. Specifically we compare the electron flux at the wall, electron-energy spectra, heat loads and the spatial distribution of the electrons for two different bunch spacings, with variable magnetic fields, and for several chamber temperatures and associated surface conditions. The simulations employ a modified, improved version of the ECLOUD code. The main changes are briefly described. We finally present updated simulation results for the heat load in the cold LHC arcs.

INTRODUCTION

The electron cloud build up is a potentially serious problem for the LHC. One main difficulty is that the electrons impacting the beam pipe in the cold part of the LHC might create a heat load that is larger than the capacity of the cryogenic cooling system. The heat load in LHC is predicted by simulations using the code ECLOUD. In order to improve the reliability of these predictions a number of benchmarking experiments were performed in the SPS. In the following some of the main results of these benchmarking studies are presented.

SIMULATION CODE

A code to simulate the electron cloud build up has to model the following components: (1) the generation of the source electrons (by ionization or synchrotron radiation hitting the beam pipe); (2) the electromagnetic fields generated by the beam and the electron cloud itself; (3) the motion of the electrons in these fields and a potential external magnetic field; and (4) the interaction of the electrons with the wall and the secondary electron generation. In ECLOUD the modelling of the secondary electron generation has been modified by taking into account the possibility that very low energy electrons may be reflected at the chamber wall with a probability near unity [1]. More details of the model used can be found in [2]. Further, the modelling of the electron motion has been improved in speed by about an order of magnitude; this allows higher precision. The modelling has also been refined by allowing the secondary emission yield to be a function of the surface position. This allows simulation of the time evolution of the surface conditioning (‘scrubbing’). In addition to these changes, many modules of the code were scrutinized and a number of bugs have been removed. In some cases this led to a significant change of the results.

ENERGY SPECTRUM

The electron momentum spectrum normal to the wall was measured at two detectors, by scanning a bias voltage and computing the differential change in the detected electron flux. Figure 1 shows experimental and simulated spectra for one of the two detectors [3], mounted vertically on a rectangular chamber with half apertures of about 64.5 mm and 24.7 mm. Installed in the SPS tunnel, this detector did not record any electrons with momenta below about 30 eV, for unknown reasons (magnetic stray field?). For the purpose of comparison, we thus removed such electrons from the simulation result. In the righthand picture, we present the simulated total-energy spectrum, for all electrons with a vertical momentum above 30 eV. The purely vertical momentum spectrum, not displayed, shows a sharp peak at the introduced artificial cutoff, and does not resemble the measurement. A possible reason could be that the real acceptance of the detector is a more complicated function in the 6-dimensional electron phase space, and not a sharp border in vertical momentum. Regardless of these uncertainties, the maximum electron energy simulated is consistent with the measurement. Energy spectra were also measured with a second ’strip’ detector and a benchmarking comparison with simulation was presented in [2]. The absolute values of the flux are often higher in the simulations than in the measurements for which calibrations are available, by factors ranging between 1 and 10. The agreement gets better as more detector effects are taken into account [2].

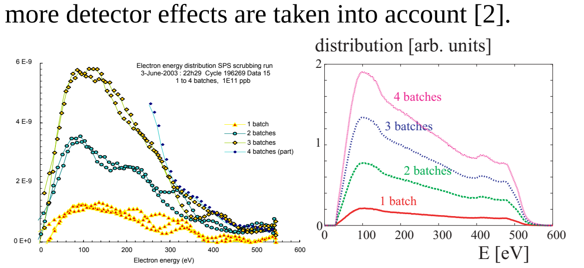

Figure 1: Electron energy spectrum for 1 to 4 batches. Left: energy spectrum measured with a variable bias voltage on the first day of the 2003 scrubbing run. Right: simulated full energy spectrum of incident electrons for $\delta_{\rm max} = 1.4$, with a vertical momentum cutoff at 30 eV.

An estimate of the heat load was derived from the measured vertical momentum distribution and the absolute flux at the wall for two different periods in the scrubbing run [3]. Figure 2 compares the estimate of the ’normal heat load’ so obtained, as a function of the number of batches, with a simulation of the same quantity. The initial vertical heat load agrees with that simulated for $\delta_{\rm max} \approx 1.4$. The dependence on the batch number is linear both in the experiment and in the simulation.

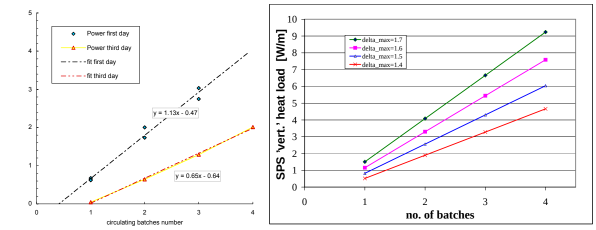

Figure 2: Left: evolution of the deposited power in W/m inferred from the vertical momentum spectrum measured during the 2003 scrubbing run with $N_b = 10^{11}$ protons. Right: simulation of the same measurement.

CALORIMETRIC MEASUREMENT

More reliable numbers for the heat load come from direct calorimetric measurements, without ambiguity in the detector acceptance. In the SPS, several calorimeters are installed [4], whose purpose is to detect the heat load deposited by electrons impinging on the chamber wall, a critical effect for the LHC. WAMPAC1 is a warm copper calorimeter with a large round chamber (70 mm radius). WAMPAC3, a similar calorimeter, has about two times smaller transverse size (33.5 mm radius). So does COLDEX, an instrumented cold vacuum chamber with a beam screen at 13–20 K.

Figure 3 shows the simulated heat load in WAMPAC1 as a function of the secondary emission yield for a bunch spacing of 25 ns and a bunch intensity of 1.15×10^{11} protons, assuming the estimated vacuum pressure of 100 nTorr. The measured value, also indicated, is consistent with $\delta_{\rm max} \approx 1.5$, the value also expected from a direct in-situ measurement of the secondary emission yield [5] at a different location in the SPS. For a larger bunch spacing of 75 ns, a detectable heat load was neither predicted by the simulations for 3 batches and $\delta_{\rm max} < 1.75$, nor measured in the experiment (resolution limit 20 mW/m). For both COLDEX and WAMPAC3 a similar agreement was found with a secondary electron emission yield of $\delta_{\rm max} = 1.3$ for a bunch spacing of 25 ns. At a spacing of 75 ns the heat load in COLDEX is less than 0.1 W/m, whereas a still significant heat load in WAMPAC3 could be explained only by $\delta_{\rm max} = 2.3$. This WAMPAC3 result for the 75-ns spacing contradicts the much lower number fitted for the 25-ns spacing and also the in-situ measurements of $\delta_{\rm max}$. A possible explanation is the existence of another unidentified heat source, one unrelated to the electron cloud, e.g., heating by trapped modes.

ELECTRON REFLECTION

If an electron impacts the beam chamber with a high energy it will produce secondaries; at lower energies (few eV) it can be reflected. The simulation results show a strong dependence on the modelling of this reflection [1]. It is thus necessary to constrain it by experiment. A potential way is to use a particularity of the SPS. The beam consists of several trains of bunches, which are usually separated by 225 ns. It can be observed that in some cases the electron

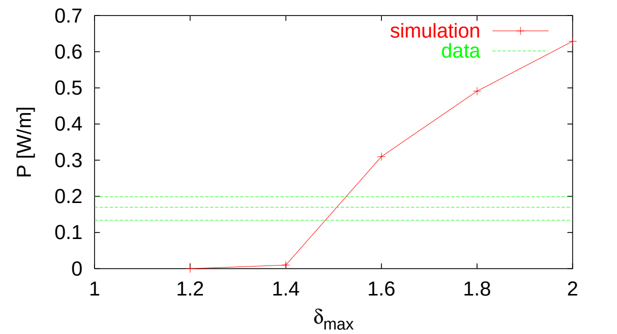

Figure 3: Simulated heat load in WAMPAC1 with 2 batches and 25-ns spacing as a function of $\delta_{\rm max}$ together with the heat loads from three consecutive measurements in 2002, indicated by straight lines.

flux at the beam pipe is increasing from one batch to another. This happens, if the cloud density does not reach the level at which it saturates due to the cancellation of space charge forces of the beam and the cloud itself. In this case some of the electrons produced during the passage of the first train can still remain in the beam chamber when the second train arives. They will thus seed the electron cloud build-up in the second train. The number of electrons which survive the gap between the bunch trains depends significantly on the gap length and on the reflectivity of the surface. By modifying the distance between the trains one can thus measure the electron reflectivity.

This measurement has been performed this year in the SPS. For a bunch spacing of 75 ns and an intensity close to the nominal LHC value it was found that a significant electron flux existed for four bunch trains and the nominal 225-ns distance between trains. Increasing the train distance to 550 ns reduced the activity strongly while at 1050 ns it became invisible. Simulations using $\delta_{\rm max} = 1.7$ (the value expected at this moment in time) and a reflectivity of 1 could reproduce this behaviour — see Fig. 4. For $\delta_{\rm max} = 1.5$ no build up along the four bunch trains is predicted by the simulation. For $\delta_{\rm max} = 1.9$ the electron cloud reaches saturation in the second bunch train and for all measured distances between trains a significant flux is expected. If the reflection probability at low energy is halved in the code, even for $\delta_{\rm max} = 1.9$ no electron flux should be observed.

QUADRUPOLE DETECTOR

The electron-cloud build up has been measured in the recent SPS run using an instrumented quadrupole. The measurements showed a very strong dependence of the electron cloud flux pattern at the chamber wall on the magnetic field. For a low magnetic field a single stripe centered between adjacent poles was observed. As the field increased from about 0.06 T/m to 0.12 T/m this stripe disappeared and two stripes developed around each pole face. For even higher fields (up to 0.6 T/m) each pair of stripes merged into a single stripe in the centre of the pole face. This observation is well reproduced in the simulations — see Fig. 5.

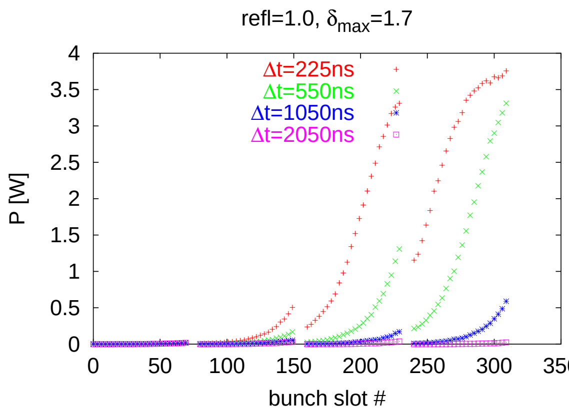

Figure 4: The build up of the electron cloud along the four bunch trains in the SPS for different distances between trains and a bunch spacing of 75 ns.

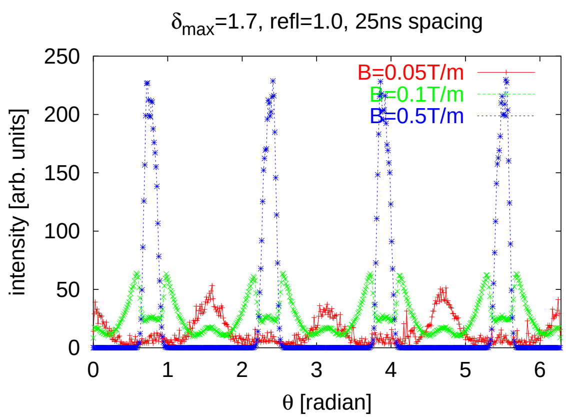

Figure 5: The simulated azimuthal distribution of the electron flux in a quadrupolar field for nominal LHC beam. The flux for 0.05 T/m was multiplied by a factor 1000.

PREDICTIONS FOR LHC

As mentioned above one of the main concerns for the LHC is the power deposited by the electrons on the beam screen that may exceed the cooling capacity of the cryogenics system. With the latest version of the code the heat load expected in the LHC has been calculated at injection and top energy, as shown in Figs. 6 and 7. It is interesting to note that, in particular at injection energy, the electron cloud does not reach its saturation level during the passage of a single bunch train, but only over a few subsequent trains. For the 75 ns bunch spacing (not displayed) the heat load remains acceptable even for the expected initial level of secondary emission yield, prior to scrubbing.

CONCLUSION

Both measurements and simulation codes were extended and refined. For realistic values of the secondary emission yield, the agreement between simulation and experimental results is good for the heat load and excellent for the spatial structure of the cloud as well as for the build-up and decay characteristics along a bunch train and between successive trains. It is only fair for the energy spectrum and the absolute flux. Analysis of the latter two requires an accurate model of the detector effects, which may explain why the agreement is not as good as for the other quantities. The benchmarking of the time evolution supports the hypothesis that low-energy electrons are reflected at the chamber wall with a high probability. If we extrapolate the heat load of 1.4 W/m measured by COLDEX for 25-ns spacing and 4 batches at the SPS in 2004, by multiplying with the ratio of filling factors (2.3), we estimate a heat load of about 3 W/m for the nominal beam at injection into the LHC; this scaling ignores the effect of differences in chamber dimensions and bunch length.

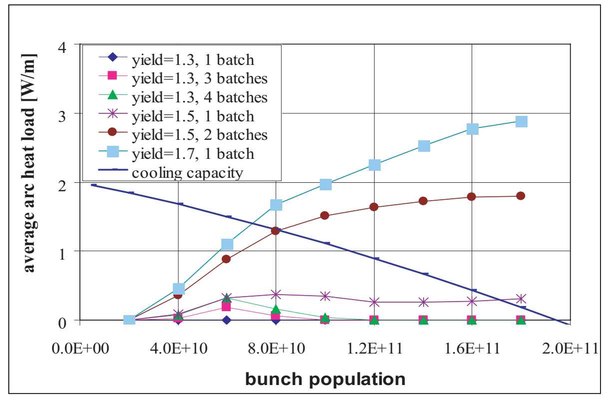

Figure 6: Simulated average arc heat load as a function of the bunch population for a bunch spacing of 25 ns at injection (450 GeV), considering various values of $\delta_{\max}$ and computing the heat load over several numbers of consecutive 72-bunch trains. An estimate of the available cooling capacity is also shown.

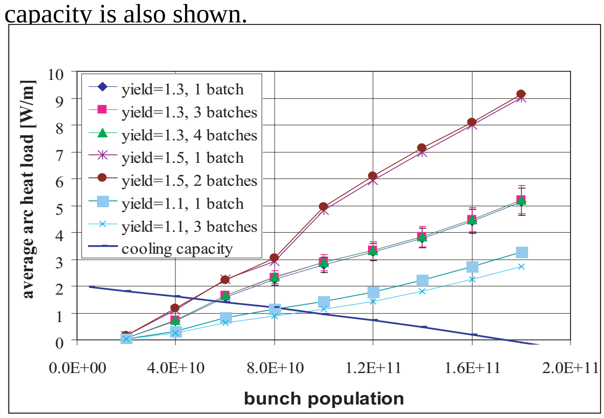

Figure 7: Simulated average arc heat load as a function of the bunch population for a bunch spacing of 25 ns at top energy (7 TeV), considering various values of $\delta_{\max}$ and computing the heat load over several numbers of consecutive 72-bunch trains. An estimate of the available cooling capacity is also shown.

REFERENCES

[1] R. Cimino, I.R. Collins, et al., CERN-AB-2004-012 (2004).
[2] D. Schulte, F. Zimmermann, ECLOUD'04 Napa (2004).
[3] J.-M. Laurent, H. Song, CERN Vacuum TN 04-02 (2004).
[4] V. Baglin, B. Jenninger, Proc. ECLOUD'02, CERN, Geneva, Switzerland, CERN-2002-001 (2002).
[5] J.M. Jimenez et al., CERN LHC Project Report 632, Proc. ECLOUD'02, CERN, Geneva, CERN-2002-001 (2002).